

Reduction behaviour of iron ores by H₂ at multi-stage reduction



Seongkyu CHO, Seong-Jin KIM , Leonardo TOMAS DA ROCHA and Sung-Mo JUNG

March 11, 2026

Chapter I. Introduction

1. Research purpose and scope

2. Research background

2.1. Traditional ironmaking process and CO₂ emissions

2.2. Alternative processes for achieving carbon neutral

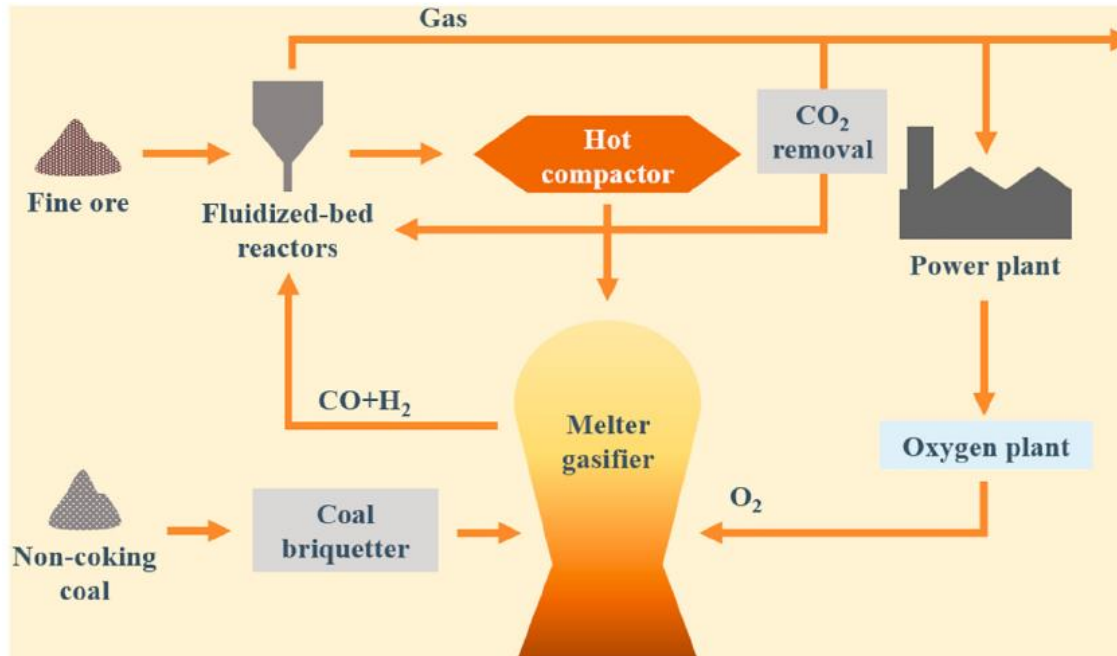
2.3. Reduction behavior of iron oxides with hydrogen as reducing agent

1. Research background

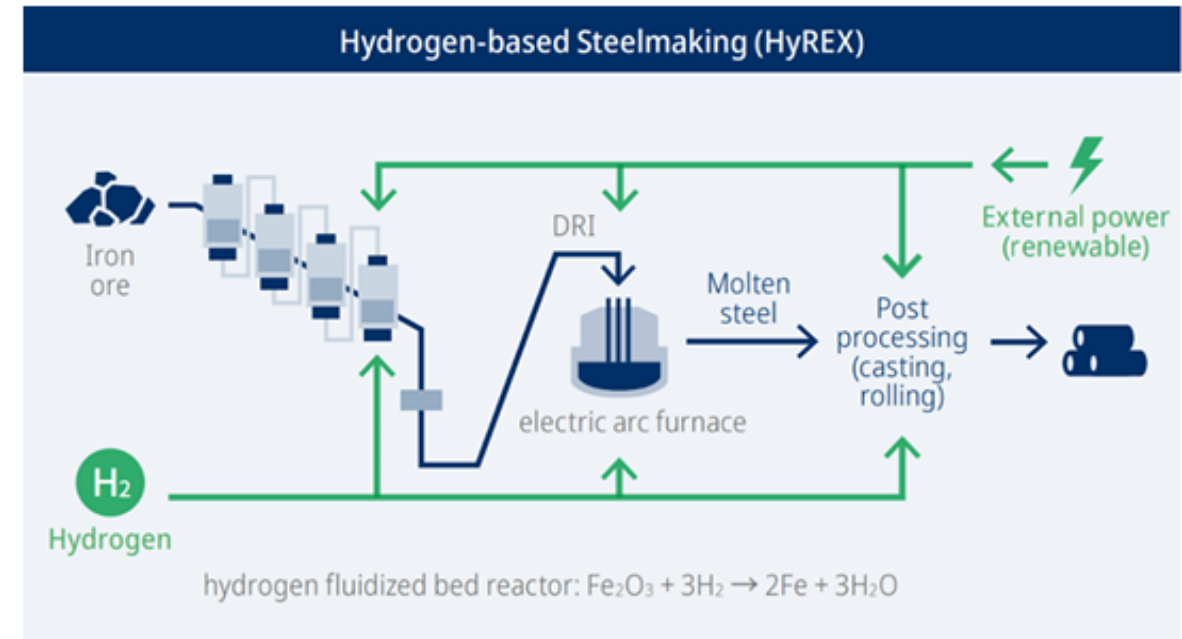
1.1. Alternative processes for achieving carbon neutral

[Zhao 2020][POSCO report]

□ Fluidized bed reduction process



FINEX process



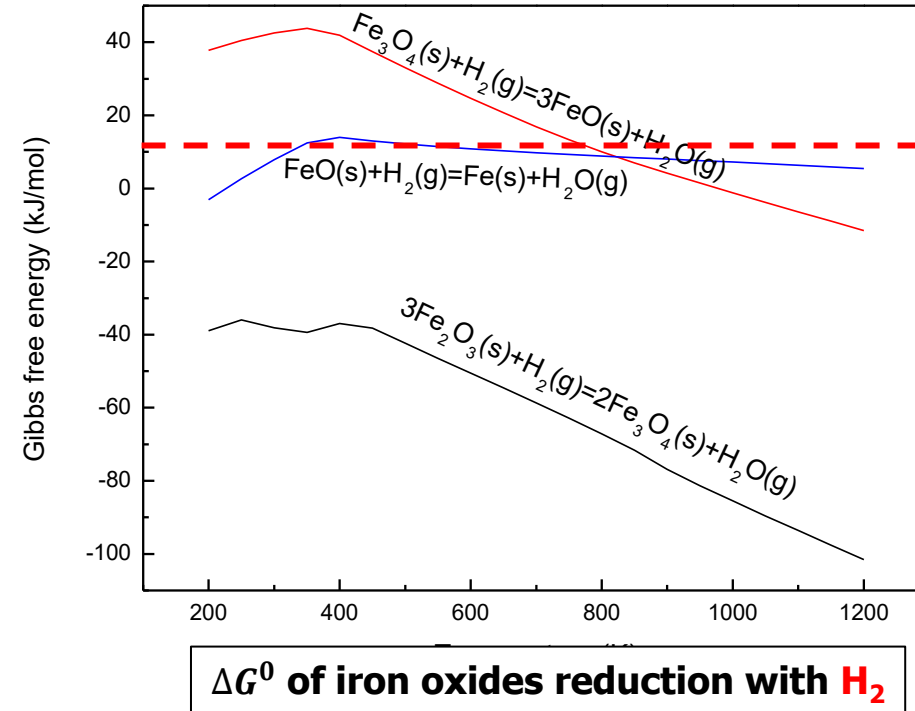
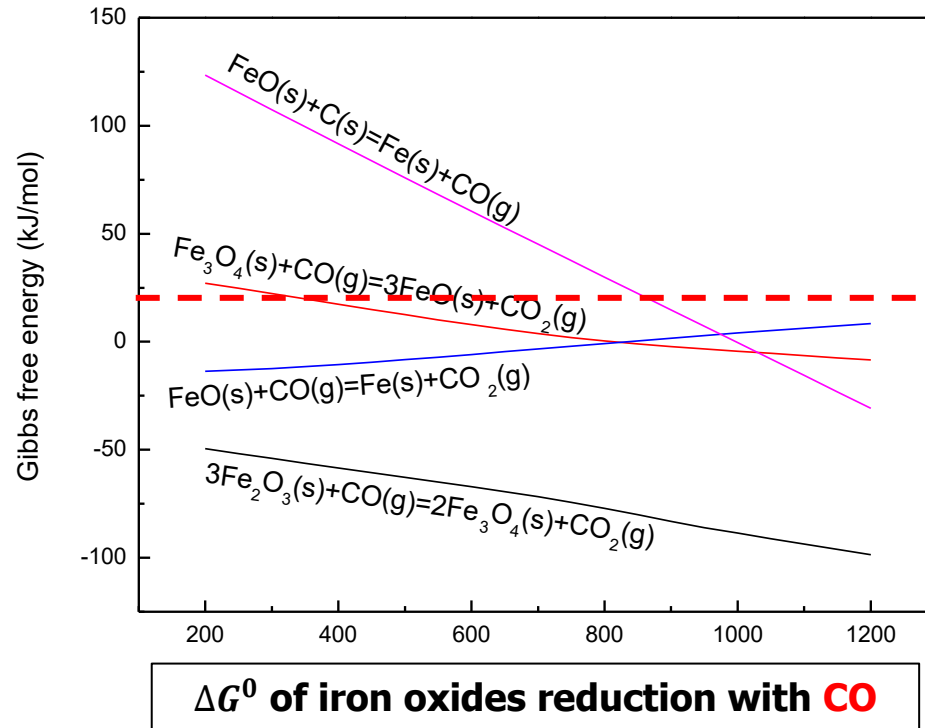
HyREX process

- ✓ **Fluidized bed reduction** processes include **FINEX** and **HyREX**. These processes offer the **advantage of using fine iron ores without the pre-treatment** such as **pelletizing or sintering**.
- ✓ However, these processes require a **large amount of hydrogen gas relative to the amount of iron ore** charged **to fluidize** the ore and show **low utilization degree of hydrogen for reduction**.

2. Theoretical background

1.2. Comparison of reduction behavior between CO and H₂

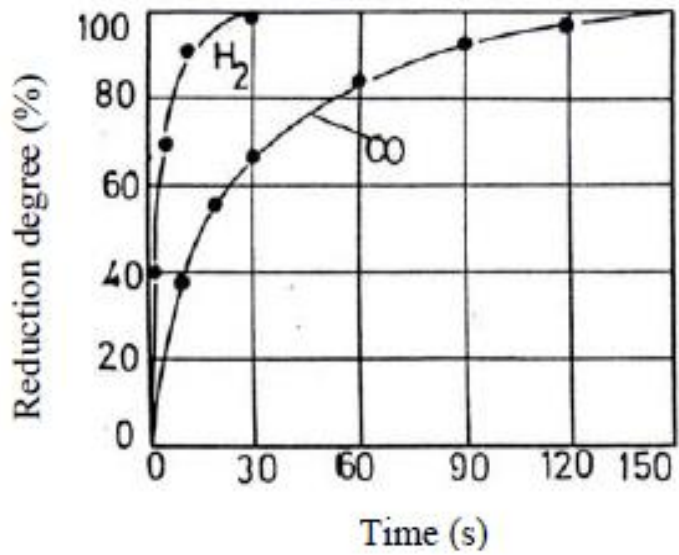
□ Iron ore reduction by **CO** and **H₂**



- ✓ In the **high temperature** range, **reduction of Fe₂O₃ and Fe₃O₄** with **CO** gas shows **negative values** of Gibbs free energy of reaction.
- ✓ In the case of reduction of **iron oxides using hydrogen**, the reduction of wustite shows a **positive Gibbs free energy of reaction**, indicating that the **utilization degree of hydrogen might be very low**.

2. Theoretical background

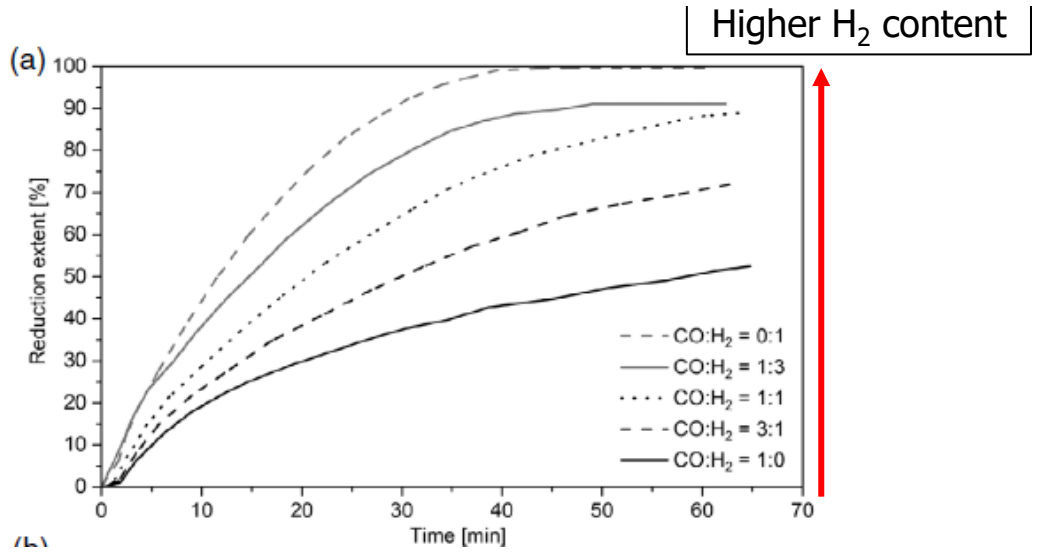
Comparison of reduction rate between CO and H₂



Comparison of reduction rate between CO and H₂

1.2. Comparison of reduction behavior between CO and H₂

[Komatina 2017][Spreitzer 2019]



Change in reduction rate with different H₂ content

✓ Reduction by H₂ showed a faster reduction rate compared to CO, suggesting that H₂ has a stronger reducing power than CO.

- When the two gases were mixed, the reduction rate also increased as the hydrogen content increased.

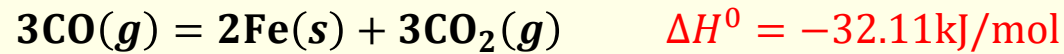
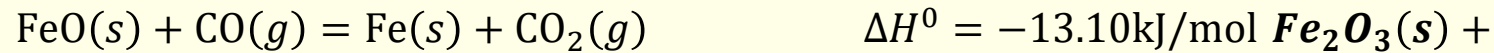
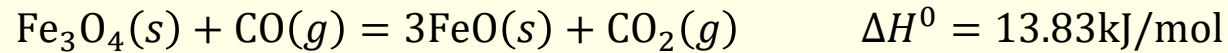
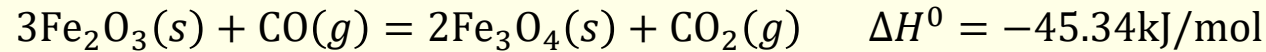
2. Theoretical background

1.2. Comparison of reduction behavior between CO and H₂

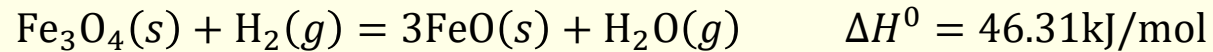
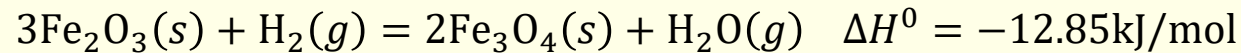
[Patisson 2020]

□ Enthalpy change during reduction

- Reduction of iron oxides using **CO (1200 K)**



- Reduction of iron oxides using **H₂ (1200 K)**



- **Fe₂O₃(s) + 3H₂(g) = 2Fe(s) + 3H₂O(g) ΔH⁰ = 65.36kJ/mol**

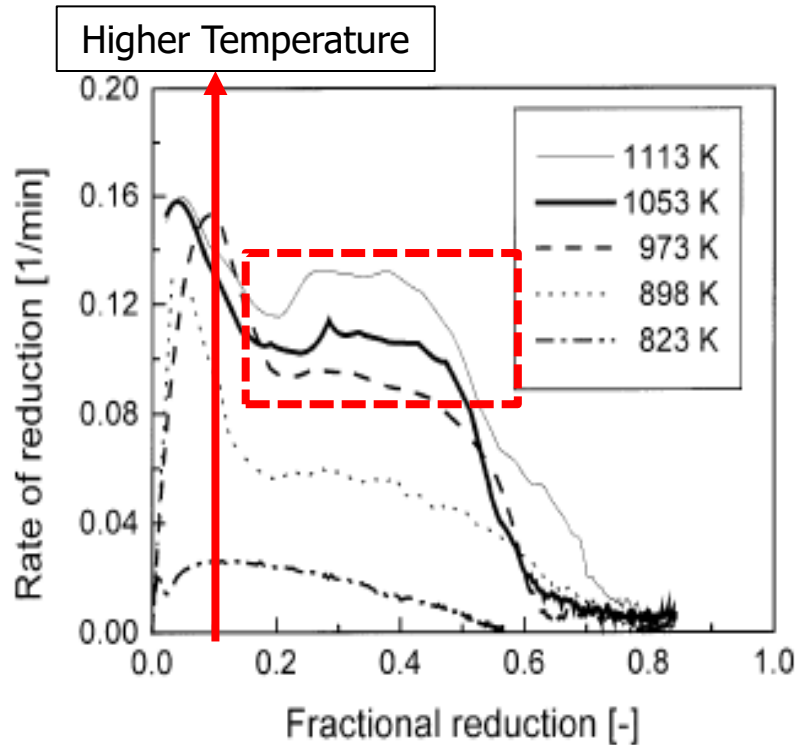
- The **reduction** using **H₂** is **endothermic**, whereas the reduction using **CO** is **exothermic**.
 - This difference led to **variation** in the **temperature** and **reduction degree** distribution within shaft furnace.

2. Theoretical background

1.3. Effect of reduction conditions on H₂ reduction

[Habermann 2000]

□ Effect of **temperature** on hydrogen reduction



Effect of temperature on the reduction rate
(55 vol% H₂, 9 vol% CO, 5 vol% CO₂, 31 vol% N₂)

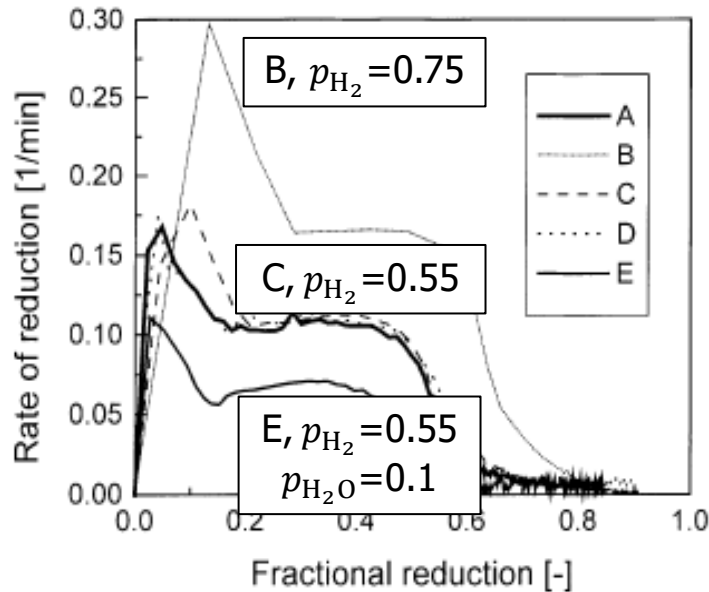
- ✓ As the **temperature increased**, the **reduction rate consistently improved**. However, this effect gradually diminished at temperature above 700 °C.
- ✓ The **reduction rate continuously varied** with the reduction degree, and the **reduction from wustite** with a reduction degree above 0.6 to metallic iron **proceeded very slowly**.

2. Theoretical background

1.3. Effect of reduction conditions on H₂ reduction

□ Effect of **gas composition** on hydrogen reduction

[Habermann 2000]



Effect of reducing gas composition on the reduction rate of hematite at 1 bar and 830 °C

A: $p_{\text{H}_2}=0.55$ bar, $p_{\text{CO}}=0.09$ bar, $p_{\text{CO}_2}=0.05$ bar,

B: $p_{\text{H}_2}=0.75$ bar,

C: $p_{\text{H}_2}=0.55$ bar,

D: $p_{\text{H}_2}=0.55$ bar, $p_{\text{CO}}=0.09$ bar, $p_{\text{CO}_2}=0.05$ bar, $p_{\text{CH}_4}=0.06$ bar

E: $p_{\text{H}_2}=0.55$ bar, $p_{\text{CO}}=0.09$ bar, $p_{\text{CO}_2}=0.05$ bar, $p_{\text{H}_2\text{O}}=0.1$ bar

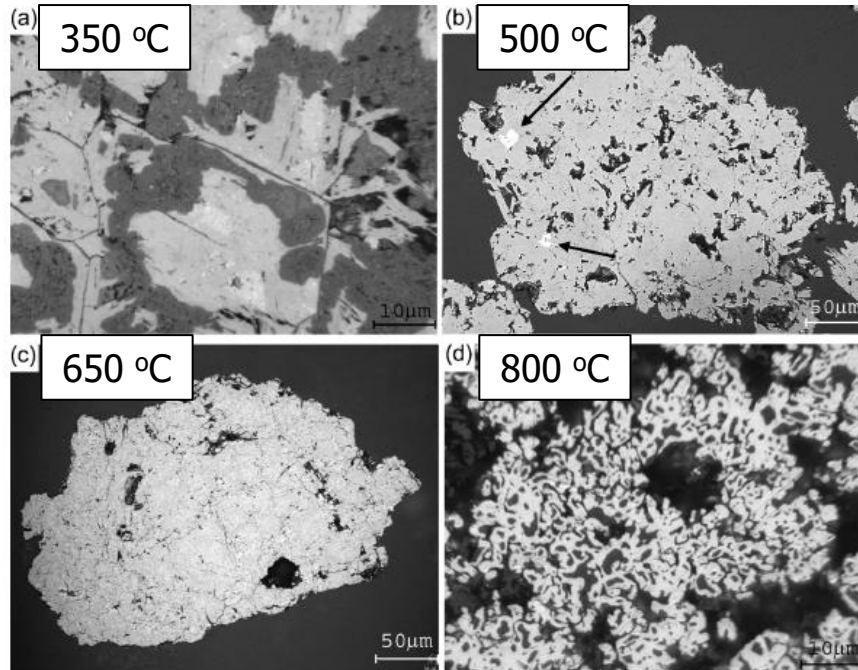
Balanced by N₂

- ✓ The comparison between **A and C** allows for the analysis of effect of **small amount of CO addition** on the reduction behavior. The **reduction rate showed little to change**, suggesting that a small amount of CO does not significantly impact H₂ reduction.
- ✓ In the case of **D**, both **CO and CH₄ were added**, but **no significant change** in the reduction rate was observed.
- ✓ Experimental condition **E** is expected to one of the most significant results. In this case, **small amount of H₂O**, which is a product of H₂ reduction, **significantly impacts** the reduction reaction. Therefore, in operation setting, **adjusting the ratio of H₂ and H₂O is to be crucial** in determining the reduction rate

2. Theoretical background

□ Effect of **pre-reduction** on hydrogen reduction

[Thurnhofer 2005]



Microstructures of reduced iron ore during pre-reduction stage at different temperature.
(a) 350 °C, (b) 500 °C, (c) 650 °C, and (d) 800 °C

- ✓ In **Figure (b)**, where the **temperature was increased to 500 °C**, the **entire iron ore was reduced to magnetite**. However, the **dense microstructure** appears to have resulted in a **lower final reduction degree**.
- ✓ When the temperature was **further increased**, leading to the **formation of wustite**, the microstructure became as shown in Figure (c). This formation of **porous wustite** was explained as contributing to the **improvement in final reduction degree**.

CHAPTER II – Effect of reduction behavior from Fe_2O_3 to FeO on the formation of metallic Fe in multi-stage hydrogen reduction

1. Introduction

2. Experimental

2.1. Material preparation

2.2. Experimental apparatus and conditions

3. Results and discussion

3.1. Reduction degree of iron ore under multi-stage reduction

3.2. Effect of R4 residence time on the final reduction degree

3.3. Kinetics analysis

4. Conclusions

1. Introduction

➤ Backgrounds

- ✓ Compared to the FINEX process, the **HyREX process** uses **hydrogen** gas as reducing agent, resulting in a **higher reduction degree** of produced DRI.
 - It is necessary to measure the **reduction degree** achieved at **each stage** of the four-stage reduction process.
- ✓ Achieving a **high reduction degree of DRI** is one of the operation target.
 - Previous study[**Thurnhofer 2005**] have indicated that reduction conditions in **initial stage influence the final reduction degree**.

➤ Research Contents

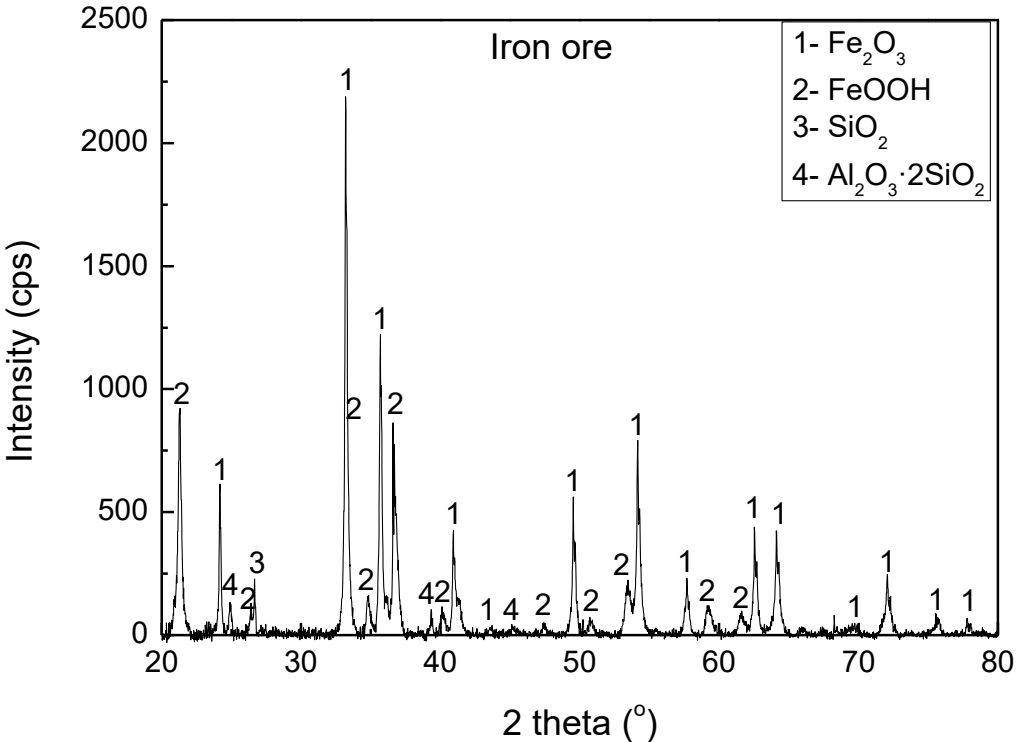
- ✓ To measure the **reduction degree** of iron ore for **each reduction stage**
- ✓ Analysis of the **residual iron oxides** after reduction
- ✓ **Improvement** of the **final reduction** degree by **varying conditions** during the **initial stage reduction**
- ✓ **Development** of strategies to enhance the final reduction degree through investigation of **reduction mechanism**

➤ Research objectives

- ✓ **Evaluation of iron ore reduction behavior under HyREX condition**

2. Experimental

Phase analysis of MAC ore



Phase composition (wt%)			
Fe_2O_3	FeOOH	SiO_2	$\text{Al}_2\text{O}_3 \cdot 2\text{SiO}_2$
61.7	32.3	3.9	2.1

✓ Fe_2O_3 and FeOOH are main phases of MAC ore.

Chemical composition of samples

Sample size: 1.4 ~ 1.7 mm

Iron ore chemical composition (wt%)											
Ore	T. Fe	FeO	SiO_2	Al_2O_3	CaO	MgO	S	P_2O_5	MnO	TiO_2	Main Phase
MAC	62.1	0.31	3.49	1.33	0.05	0.05	0.02	0.15	0.19	0.06	Fe_2O_3 + FeOOH

2. Experimental

2.1. Materials preparation

MAC ore (wt%)	
Fe ₂ O ₃	FeOOH
62	32



- ✓ **400 mg** of MAC ore
- **248 mg Fe₂O₃, 128 mg FeO(OH)**
- During **dehydration**

$$2\text{FeO(OH)}(s) = \text{Fe}_2\text{O}_3(s) + \text{H}_2\text{O}(g)$$

128 mg of FeO(OH) become 115 mg of Fe₂O₃

- ✓ After dehydration, **totally 363 mg of Fe₂O₃**
- Maximum **oxygen removal: 109 mg**

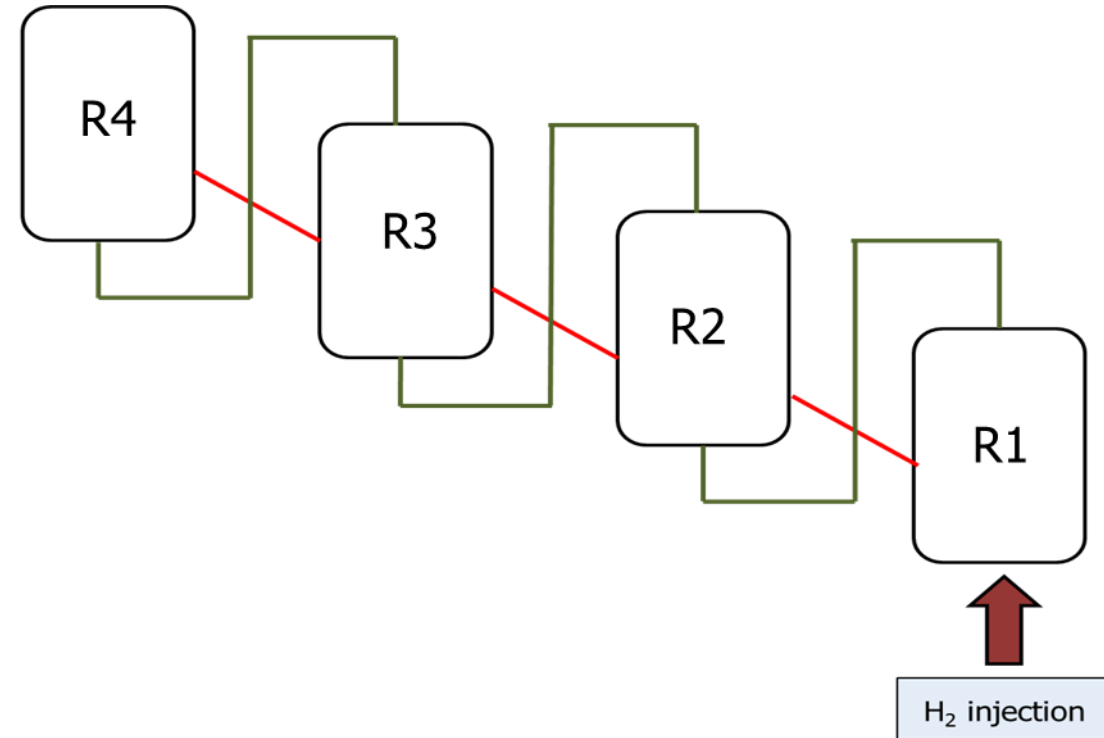
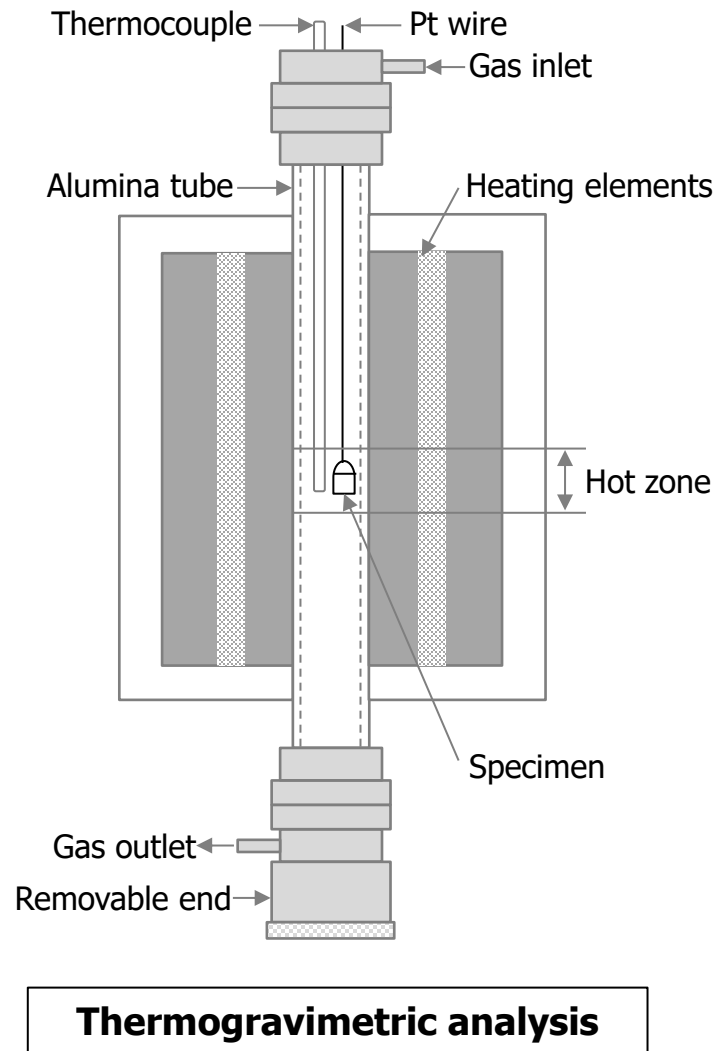
Weight loss from 400 mg MAC				
	Dehydration (~250 °C)	Fe ₂ O ₃ ->Fe ₃ O ₄ (R4)	Fe ₃ O ₄ -> FeO (R3)	FeO -> Fe (R2, R1)
Expected weight loss	13 mg	12 mg	24 mg	73 mg
Expected reduction degree	-	11%	33%	100%

✓ Based on the maximum weight loss during reduction, reduction degree was evaluated.

$$\text{Reduction degree (\%)} = \frac{\text{Weigh loss during 4-stage reduction (mg)}}{\text{Maximum weight loss with stoichiometric calculation (mg)}} \times 100$$

2. Experimental

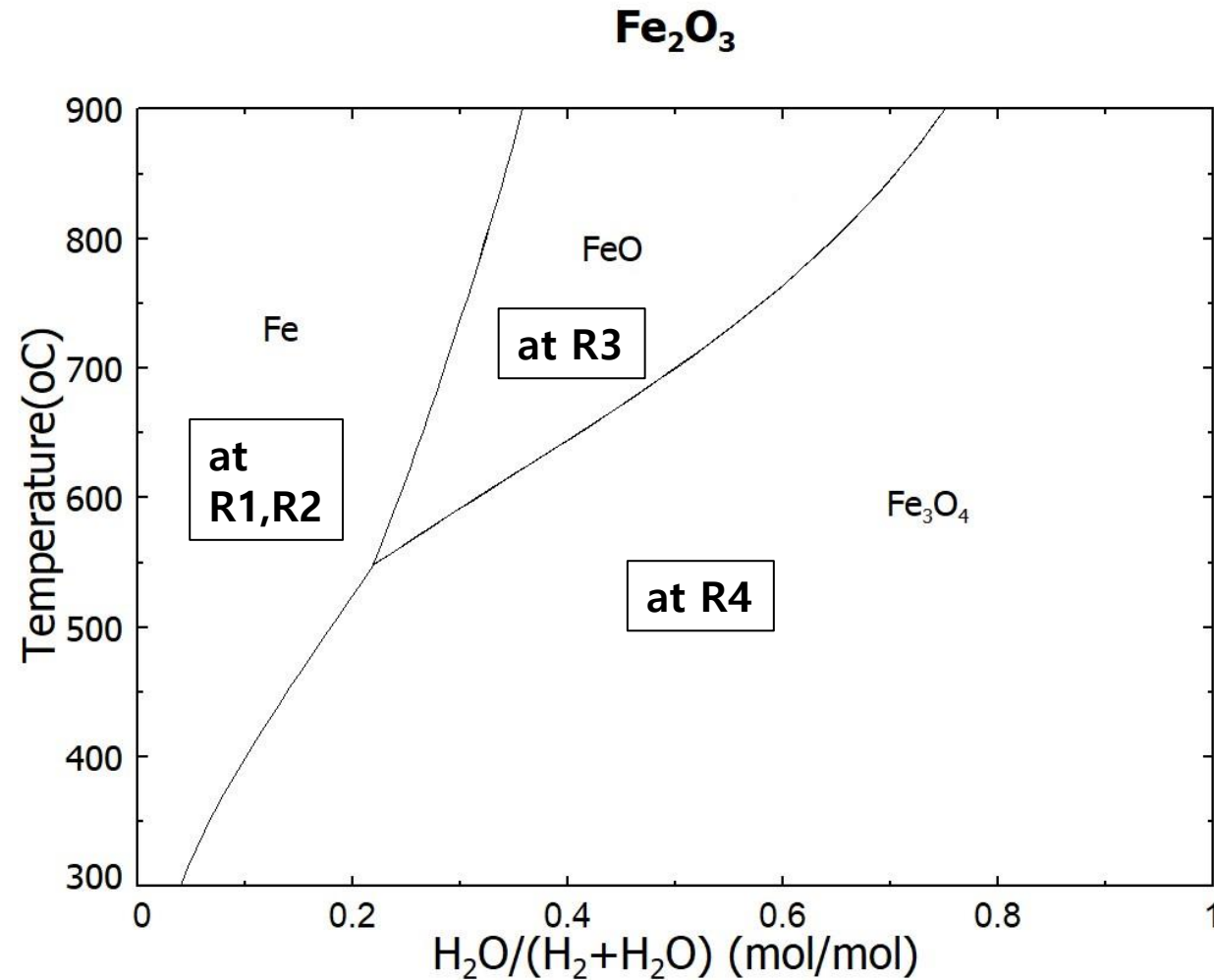
2.2. Experimental apparatus and conditions



- **Sample:** MAC, 0.4g
- **Experimental condition:** Specific conditions under R4, R3, R2 and R1
- **Total flow rate:** 1L/min

2. Experimental

2.2. Experimental apparatus and conditions



Baur-Glassner diagram and experimental conditions at four stages (FactSage)

Experimental conditions at each reduction stage				
Conditions	R4	R3	R2	R1
Temperature	450 °C	630 °C	700 °C	750 °C
H ₂ (ml/min)	600	620	670	720
H ₂ O (ml/min)	230	210	160	110
N ₂ (ml/min)	170			
Time (min)	30	30	40	40

Change of residence time at R4

at R4 (0-10 min)

at R3 (30 min)

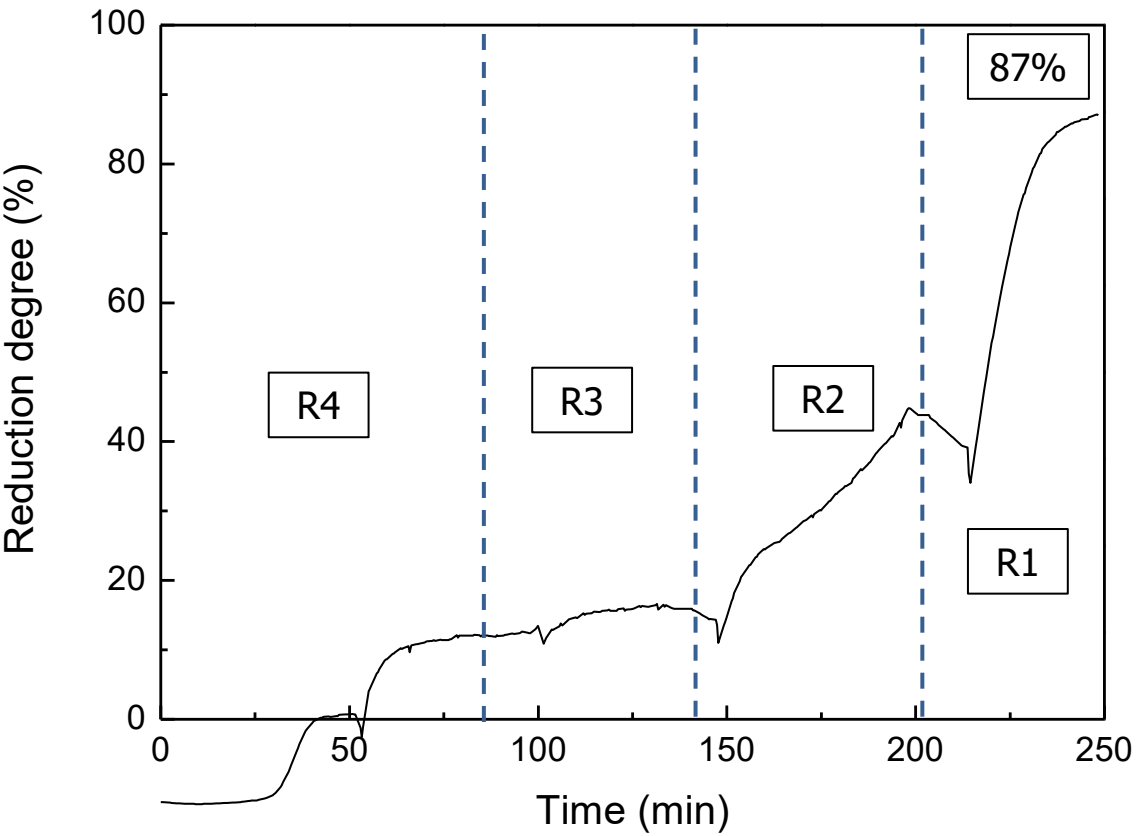
at R2 (40 min)

at R1 (40 min)

3. Results and discussion

3.1. Reduction degree of iron ore under multi-stage reduction

Reduction of MAC ore



Reduction degree (%)				
	R4	R3	R2	R1
Measured	11	16	44	87
Expected	11	33	100	

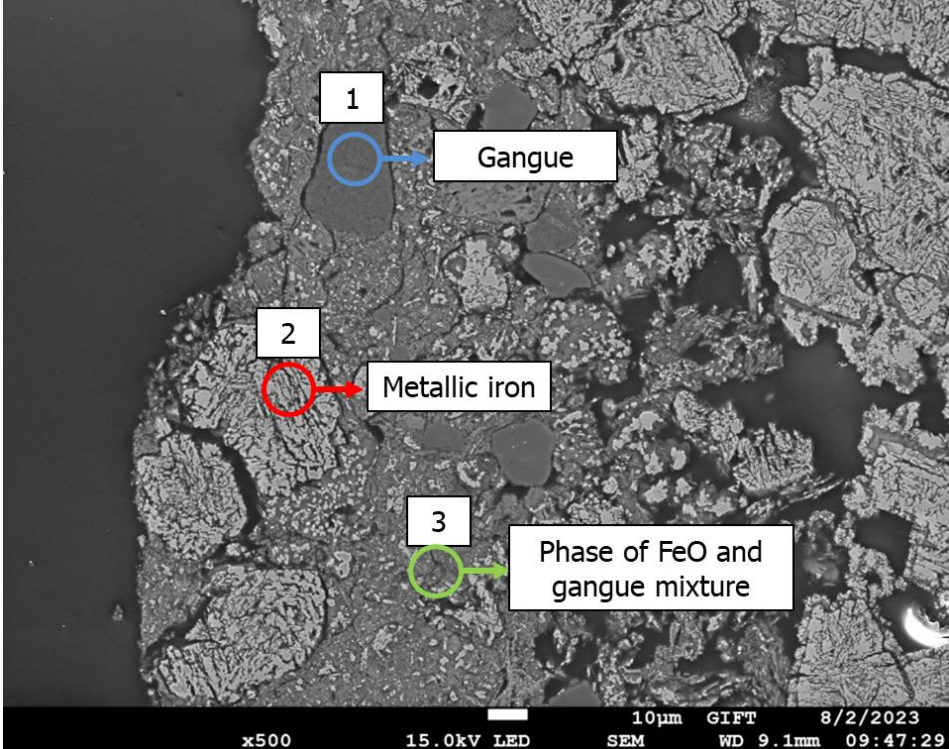
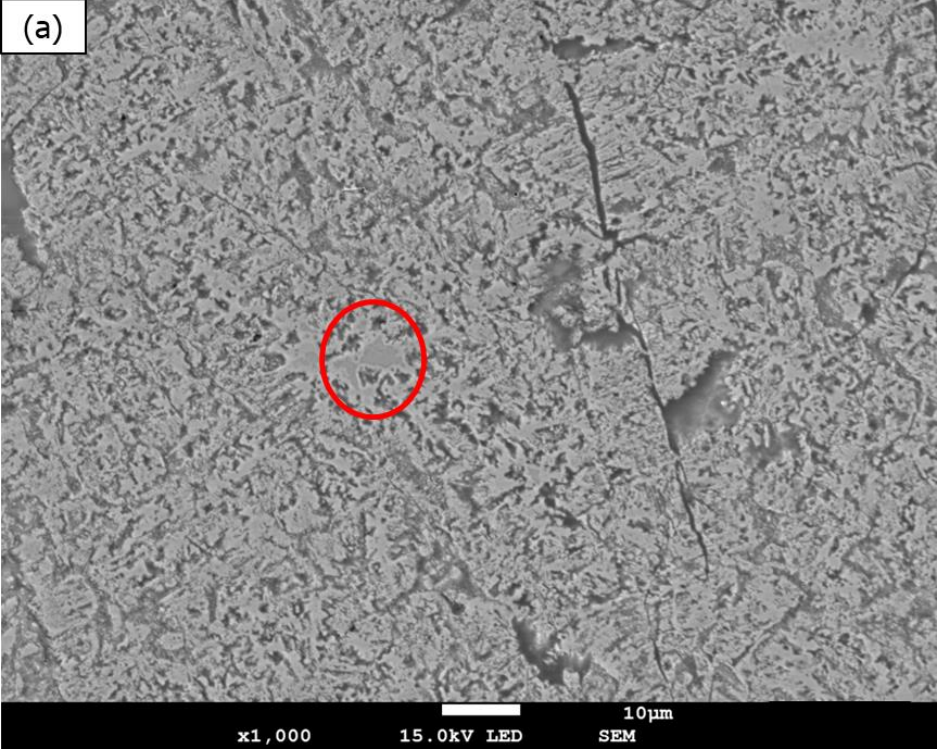
- ✓ Under standard condition, **87 % of final reduction degree** was obtained after R1 reduction.
- ✓ Within **15 min, reduction of hematite to magnetite** was finished under R4 condition.

Change in the reduction degree at four reduction stages

3. Results and discussion

3.1. Reduction degree of iron ore under multi-stage reduction

SEM image of reduced iron ore after four-stage reduction



Microstructure of iron ore after reduction (RD: 87%)

- ✓ There are two kinds of **unreduced iron oxides**.
 - **Dual phase** grain (Outer: metallic iron, Internal core: FeO)
 - **Mixed phase** of FeO and gangue

1 composition (wt%)			
Al	Si	Fe	O
23	26	3	48

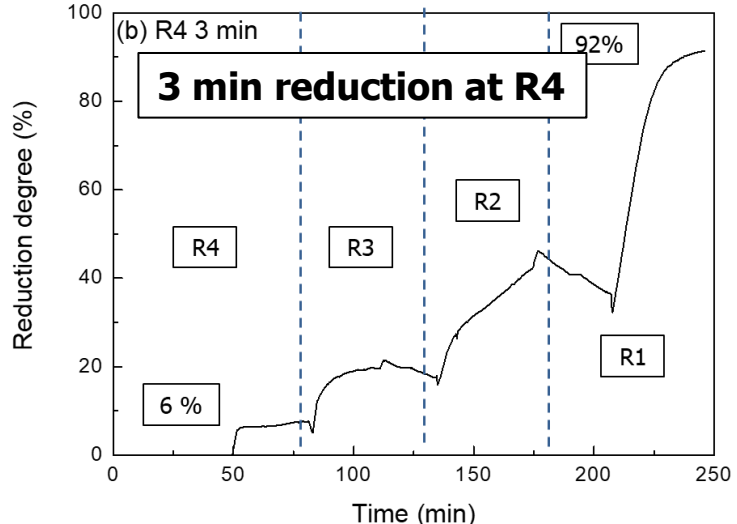
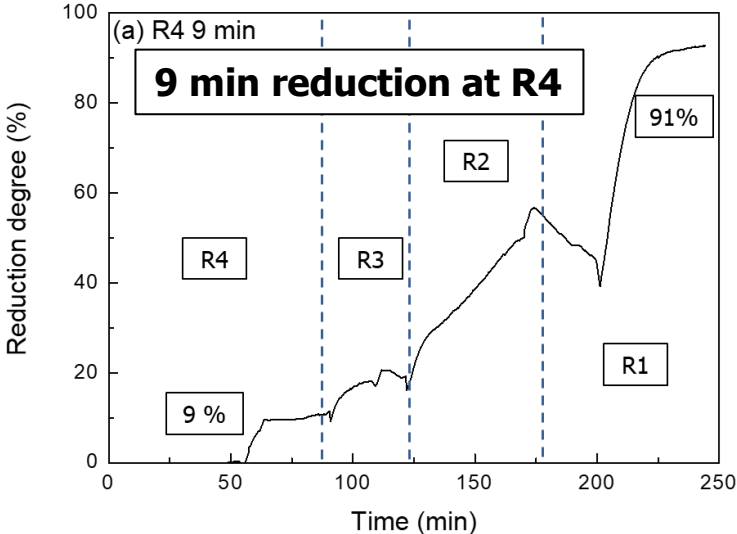
2 composition (wt%)			
Fe			
99			

3 composition (wt%)			
Al	Si	Fe	O
4	5	75	15

3. Results and discussion

3.2. Effect of R4 residence time on the final reduction degree

Control of residence time at R4 stage (Achieve different reduction degree under R4)



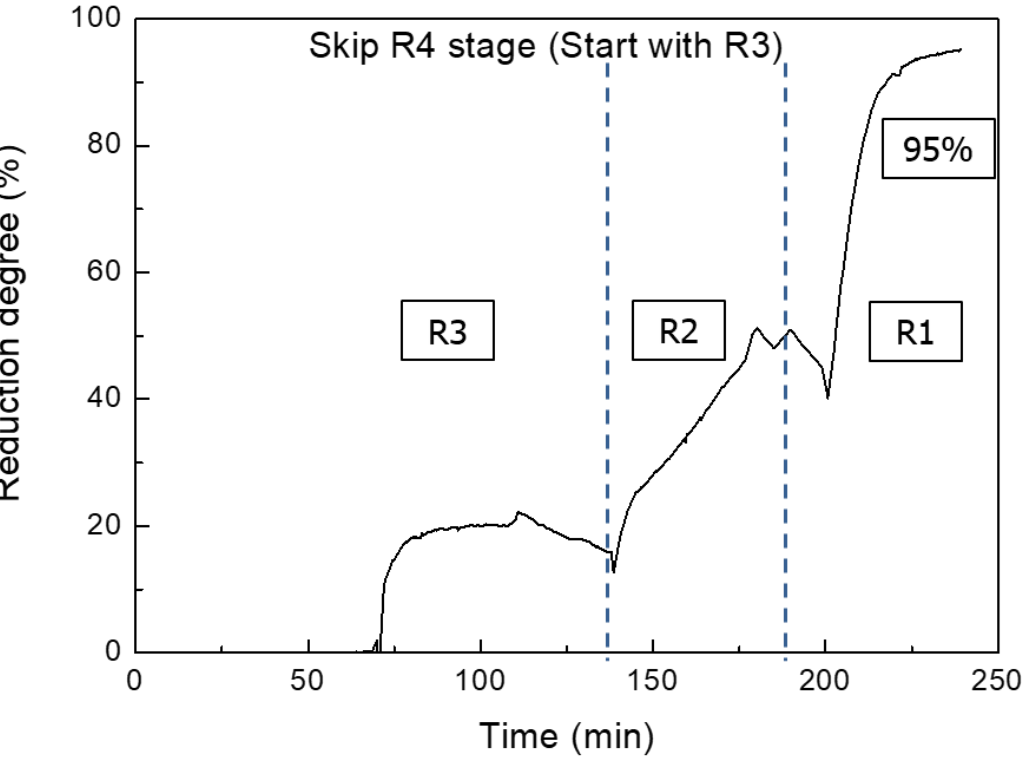
Reduction degree (%)				
Residence time at R4	R4	R3	R2	R1
30 min (Standard)	11	16	44	87
9 min	9	18	50	91
3 min	6	19	42	92

✓ When the **reduction degree become lower at R4**, **final reduction degree become higher after R1.**

3. Results and discussion

3.2. Effect of R4 residence time on the final reduction degree

Three-stage reduction (R3 → R2 → R1)



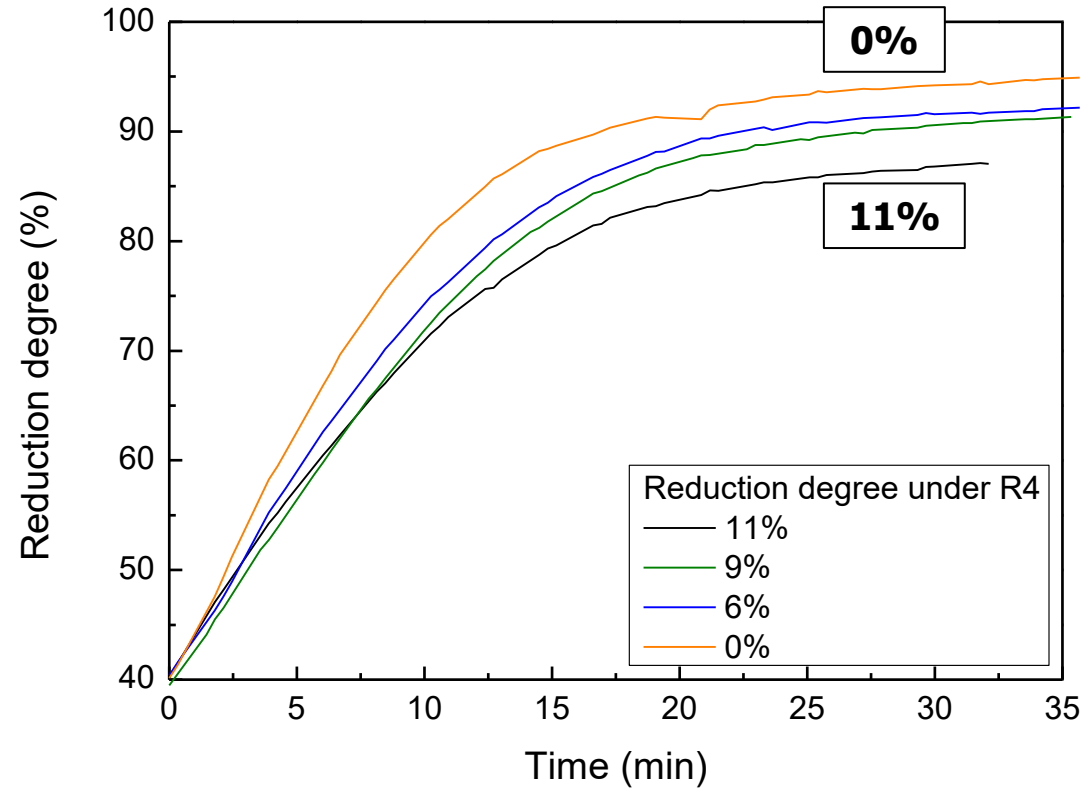
Reduction degree (%)				
Residence time at R4	R4	R3	R2	R1
30 min (Standard)	11	16	44	87
9 min	9	18	50	91
3 min	6	19	42	92
0 min (Skip)	-	21	47	95

✓ **Without R4 condition (three stage reduction), final reduction degree was evaluated to be 95%.**

3. Results and discussion

3.2. Effect of R4 residence time on the final reduction degree

Change in reduction degree during R1



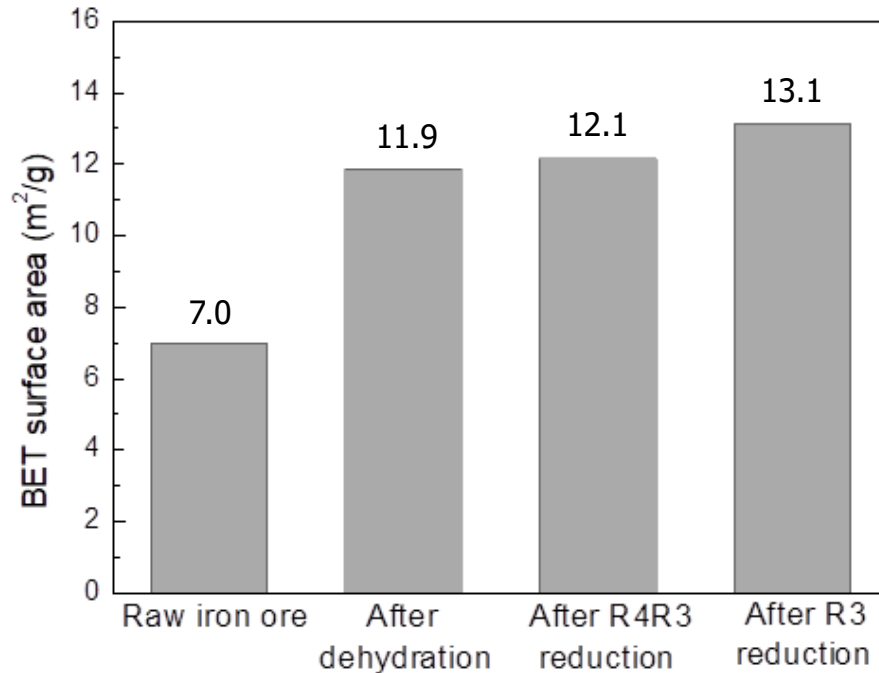
Effect of reduction degree at R4 on the final reduction degree.

✓ When analyzing the most important reaction in the iron oxide reduction which is the reduction of FeO to Fe, it was observed that **as the reduction degree decreased at R4, the degree and rate of reduction at R1 increased.**
⇒ This suggests that the initial reduction **reaction from Fe₂O₃ to Fe₃O₄ strongly affect the formation of metallic iron.**

3. Results and discussion

3.2. Effect of R4 residence time on the final reduction degree

□ Change of surface area during reduction



Surface area of raw iron ore, iron ore after dehydration, reduced iron ore at R4-R3 and R3

- ✓ The surface areas of raw and hydrated iron ores were measured to be 6.97 and 11.85 m²/g, respectively.
 - **Dehydration increased the surface area** as water **within the goethite crystal was removed.**
- ✓ The ore **reduction degrees at R4-R3 and R3 are similar (18%)**, while the **surface area** after reduction was observed **different (12.1 for R4-R3 and 13.1 for R3)**.
 - When ores were **exposed to stronger experimental conditions (temperature or reduction potential)**, it caused **faster reduction or dehydration**, which **promoted the formation of more cracks** (higher surface area).

3. Results and discussion

□ Kinetics analyses

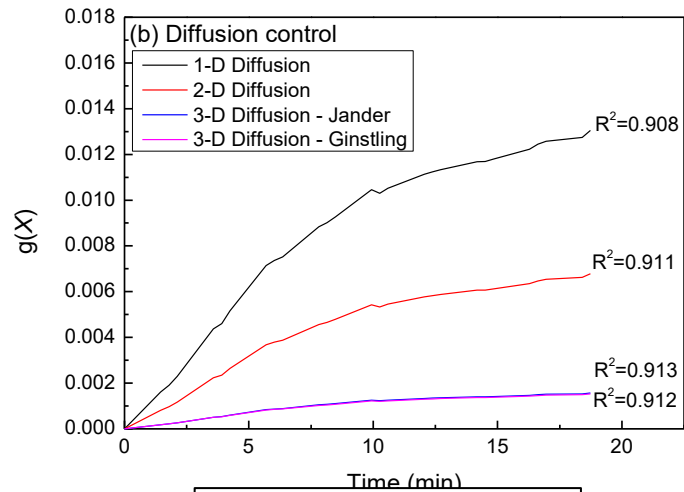
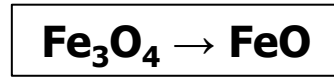
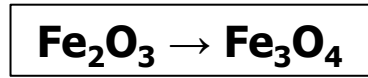
Model	$g(X) = k * t$	
Chemical reaction at interface	Mass Transport	X
	Contracting Area	$1 - (1 - X)^{1/2}$
	Contracting Volume	$1 - (1 - X)^{1/3}$
Diffusion Control	1-D Diffusion	X^2
	2-D Diffusion	$(1 - X) * \ln(1 - X) + X$
	3-D Diffusion – Jander	$[1 - (1 - X)^{1/3}]^2$
	3-D Diffusion – Ginstling	$1 - 2/3 * X - (1 - X)^{2/3}$
Reaction Control	1st Order	$-\ln(1 - X)$
	3/2 Order	$2 * [(1 - X)^{-1/2} - 1]$
	2nd Order	$(1 - X)^{-1} - 1$
	3rd Order	$1/2 * [(1 - X)^{-2} - 1]$
Nucleation	Avrami 1.5	$[-\ln(1 - X)]^{2/3}$
	Avrami 2	$[-\ln(1 - X)]^{1/2}$
	Avrami 3	$[-\ln(1 - X)]^{1/3}$
	Avrami 4	$[-\ln(1 - X)]^{1/4}$

- ✓ The **reduction mechanism** at each reduction reaction was analyzed.
- The **fitting model** provides fundamental data for improvement of the reduction degree.
 - **Diffusion** control: More surface area, Smaller iron ore size
 - **Reaction** control: Higher temperature, Higher hydrogen partial pressure

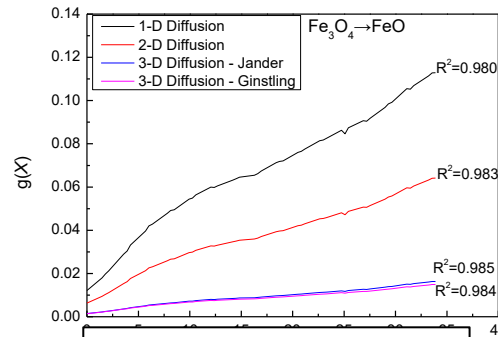
3. Results and discussion

3.3. Kinetics analysis

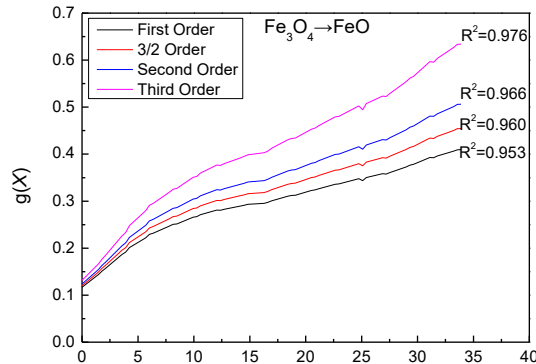
□ Kinetics analysis for each reduction reaction



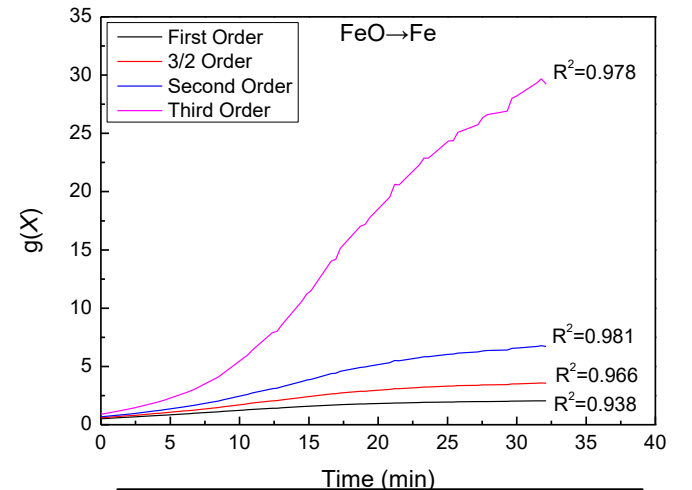
Diffusion control



Diffusion control



Chemical reaction control



Chemical reaction control

- ✓ Different kinetic mechanisms were identified for each reduction reaction, respectively.
- **Diffusion** \Rightarrow **Diffusion** and 1st order chemical **reaction (mixed control)** \Rightarrow Third order **chemical reaction**

3. Results and discussion

3.3. Kinetics analysis

Models		R ² value for each model		
		Fe ₂ O ₃ → Fe ₃ O ₄	Fe ₃ O ₄ → FeO	FeO → Fe
Phase-Boundary control Geometrical Contraction	Mass Transport	0.777	0.935	0.842
	Contracting Area	0.834	0.944	0.896
	Contracting Volume	0.836	0.947	0.911
Diffusion Control	1-D Diffusion	0.908	0.980	0.886
	2-D Diffusion	0.911	0.983	0.920
	3-D Diffusion – Jander	0.913	0.985	0.953
	3-D Diffusion – Ginstling	0.912	0.984	0.933
Reaction Control	1 st Order	0.790	0.953	0.938
	3/2 Order	0.796	0.960	0.966
	2 nd Order	0.802	0.966	0.981
	3 rd Order	0.814	0.976	0.983
Nucleation	Avrami 1.5	0.677	0.928	0.918
	Avrami 2	0.583	0.913	0.906
	Avrami 3	0.452	0.897	0.892
	Avrami 4	0.371	0.888	0.885

4. Conclusions

- ✓ Change in **reduction degree** was measured during the **four-stage hydrogen reduction** process.
 - **11% → 18% → 40% → 87%**
- ✓ **Residual iron oxides** after the reduction showed in **two types**.
 - **Dual phases grain** (Outer: metallic iron, Inside core: FeO)
 - **Mixed phase of FeO and gangue**
- ✓ As the **duration time of first reduction stage decreased**, the **final reduction degree** was **improved**.
 - Reduction in stronger reducing atmosphere at the early stage led to increase in surface area.
- ✓ **Different reduction mechanism** were identified for **each reduction** reaction.

Reduction mechanism for each reaction		
$Fe_2O_3 \rightarrow Fe_3O_4$	$Fe_3O_4 \rightarrow FeO$	$FeO \rightarrow Fe$
Diffusion control	Mixed control (Diffusion + Reaction)	Chemical reaction

CHAPTER III – Effect of iron ore type on reduction behavior at multi-stage hydrogen reduction

1. Introduction

2. Experimental

- 2.1. Material preparation
- 2.2. Experimental apparatus and conditions
- 2.3. Evaluation of reduction degree
- 2.4. Kinetics analysis

3. Results and discussion

- 3.1. Reduction behavior of four kinds of iron ores and their kinetic analyses
- 3.2. Effect of crystallite size and lattice constant on the reduction behavior of iron ores
- 3.3. Effect of SiO₂ on the reduction behavior of iron ores

4. Conclusions

1. Introduction

➤ Backgrounds

- ✓ Due to the **supply of iron ore**, it is necessary to analyze the reduction behavior of **various iron ores**.
 - Since **HyREX process does not involve pre-treatment** such as **sintering and significant variation in reduction behavior** are expected depending on the **iron ore brands**
- ✓ Analysis of effect of **iron oxide phase** (Fe_2O_3 , $\text{FeO}(\text{OH})$ and $\text{Fe}_2\text{O}_3 \cdot \text{H}_2\text{O}$) in raw ores on **reduction behavior**

➤ Research Contents

- ✓ To measure the **reduction degree of each reduction stage** for several iron ore brands
- ✓ Analysis of the **lattice parameter** and **crystallite size** of iron oxides formed during the reduction process for **iron ore brands** and **their effect** on **reduction behavior**
- ✓ To study the effect of **gangue components** on **reduction behavior**

➤ Research objectives

- ✓ **To clarify the effect of iron ore properties on reduction behavior in HyREX conditions**

2. Experimental

2.1. Material preparation

□ Chemical composition of iron ores

Titration/ICP

Sample size: 1.4 ~ 1.8 mm

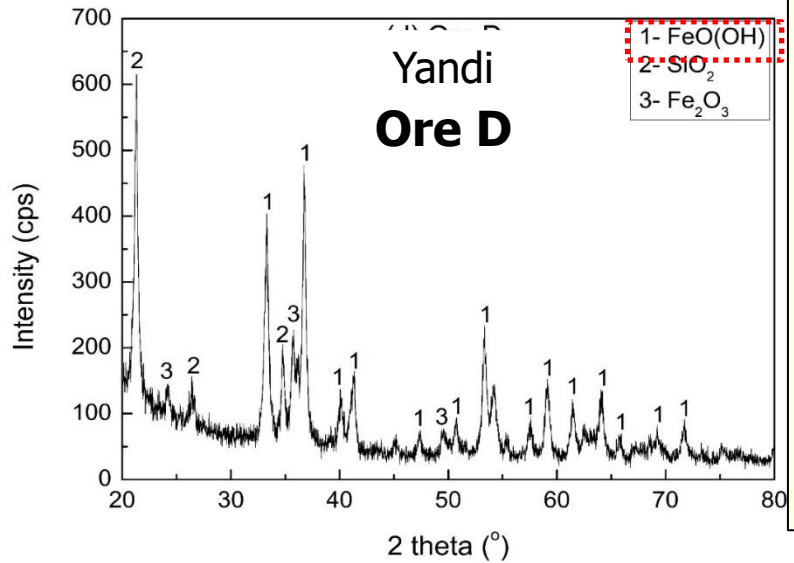
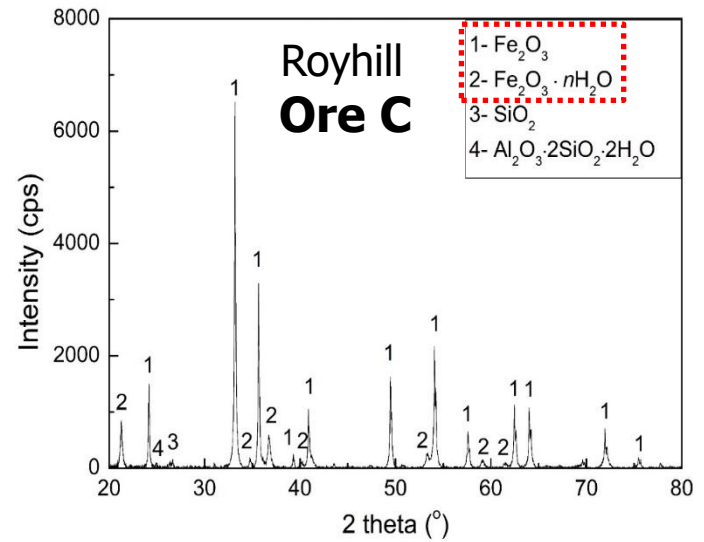
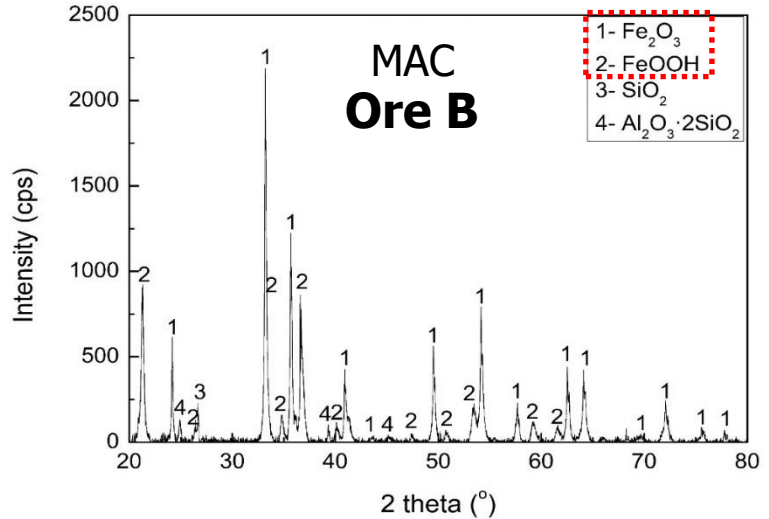
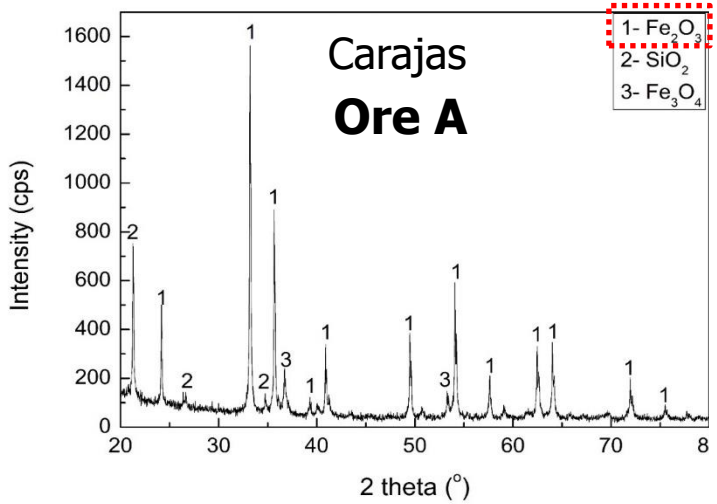
Iron ore chemical composition (wt%)									
Ore	T. Fe	FeO	SiO ₂	Al ₂ O ₃	CaO	MgO	S	P ₂ O ₅	Main Phases
Carajas (Ore A)	65.2	0.46	1.52	1.25	0.07	0.05	0.03	0.15	Fe ₂ O ₃
MAC (Ore B)	62.1	0.31	3.49	1.33	0.05	0.05	0.02	0.15	Fe ₂ O ₃ + FeO(OH)
Royhill (Ore C)	59.7	0.1	4.69	2.55	0.11	0.11	0.03	0.14	Fe ₂ O ₃ + Fe ₂ O ₃ ·H ₂ O
Yandi (Ore D)	57.0	0.17	5.39	1.59	0.06	0.08	0.06	0.08	FeO(OH)

- ✓ All of them contain **very low FeO content**, which represents **minimal presence of magnetite**.
 - Ore A is **high-grade Brazilian iron ore** with **low gangue** content and **high amount of total Fe**.
 - **Ore B, Ore C and Ore D** are **Australian iron ores** with **higher gangue content** compared with Ore A.

2. Experimental

2.1. Material preparation

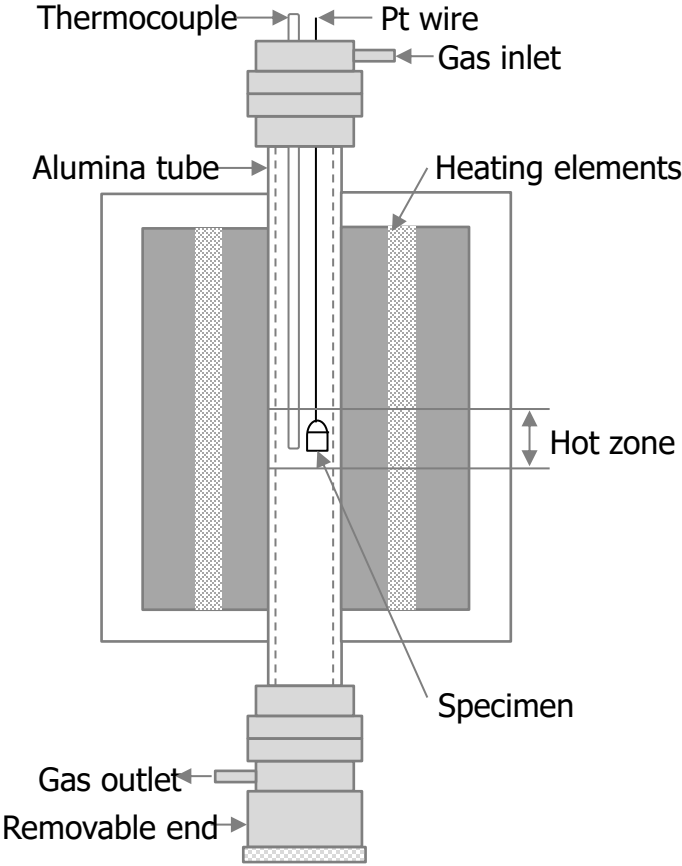
Phase identification of four iron ores



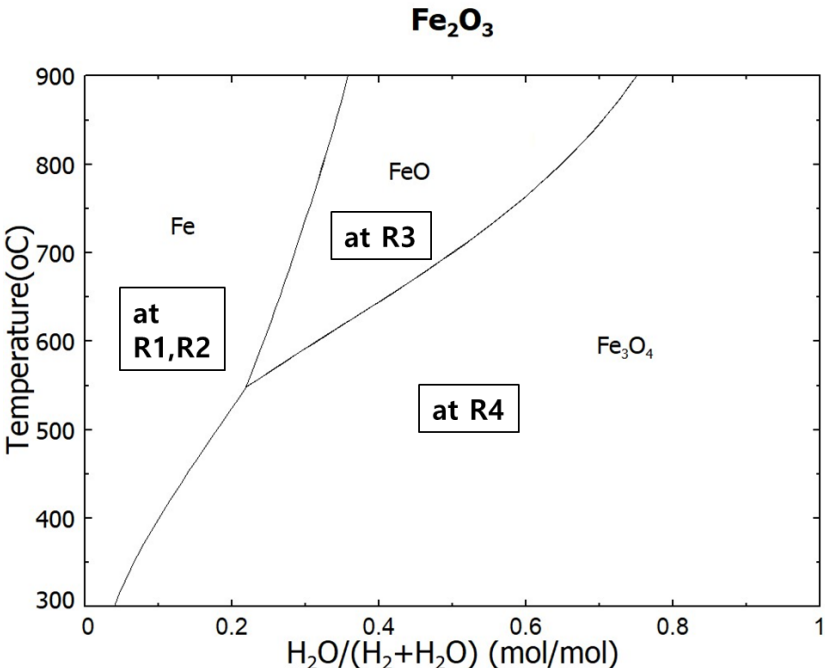
- ✓ **Fe₂O₃** in **Ore A (Carajas)** was identified to be the main phase while **Ore B (MAC)** and **Ore C (Royhill)** consist of **Fe₂O₃, FeO(OH)** and **Fe₂O₃·H₂O**.
- ✓ Lastly, **Ore D (Yandi)** was primarily composed of **FeO(OH)**.
- ✓ This indicates that **Ore B, Ore C and Ore D** would show the **weight loss due to dehydration** while heating up to target temperature.

2. Experimental

2.2. Experimental apparatus and conditions



Thermogravimetric analysis



- **Sample:** 0.4g
- **Experimental condition:** Specific conditions at R4, R3, R2 and R1
- **Total flow rate:** 1L/min

Experimental conditions at each reduction stage				
Conditions	R4	R3	R2	R1
Temperature	450 °C	630 °C	700 °C	750 °C
H₂ (ml/min)	600	620	670	720
H₂O (ml/min)	230	210	160	110
N₂ (ml/min)	170			
Time (min)	30	30	40	40

2. Experimental

2.3. Evaluation of reduction degree

Weight loss at each reduction (mg)					
Iron ores	Dehydration (~250 °C)	$\text{Fe}_2\text{O}_3 \Rightarrow \text{Fe}_3\text{O}_4$ (R4)	$\text{Fe}_3\text{O}_4 \Rightarrow \text{FeO}$ (R3)	$\text{FeO} \Rightarrow \text{Fe}$ (R2/R1)	Total weight loss by
Ore A (Carajas)	-	12	25	76	113
Ore B (MAC)	13	12	24	73	109
Ore C (Royhill)	9	11	22	69	102
Ore D (Yandi)	36	11	21	65	97
Expected reduction degree(%)	-	11%	33%	100%	

✓ Based on the maximum weight loss during reduction, reduction degree was evaluated.

$$\text{Reduction degree (\%)} = \frac{\text{Weight loss during 4-stage reduction (mg)}}{\text{Maximum weight loss with stoichiometric calculation (mg)}} \times 100$$

2. Experimental

□ Crystallite size of Fe_2O_3 and Fe_3O_4

✓ Since **iron oxide phases** are **different** within iron ores, it is expected that **crystallite size of iron oxide** might be **different** and **affect reduction behavior** in hydrogen reduction.

✓ **Crystallite** size analysis

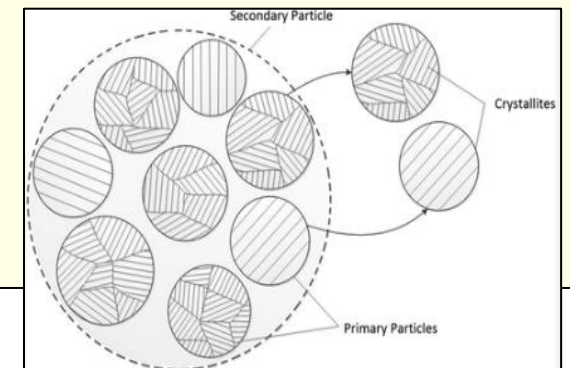
- The crystallite size was estimated by X-ray diffraction peaks with the **Scherrer formula**.

$$L = \frac{K\lambda}{\beta \cos\theta}$$

(L : crystallite size, K : a constant related to crystallite shape, normally taken as 0.9,

λ is the X-ray wavelength in 0.1506 nm (the wavelength of $K\alpha$ Cu X-ray in nanometer), β is full width at half maximum (FWHM) and θ is peak position in degree)

✓ $L = \frac{\boxed{K\lambda} \text{ Constant}}{\boxed{\beta \cos\theta} \text{ Constant}}$ [Small β (FWHM) \rightarrow Larger L \rightarrow Larger crystal size]



2. Experimental

□ Lattice constant of Fe_2O_3 and Fe_3O_4

✓ Lattice constant of Fe_2O_3 and Fe_3O_4

- The crystal structures: Fe_2O_3 (**hexagonal** closed-packed crystal), Fe_3O_4 (**cubic closed-packed** crystal)

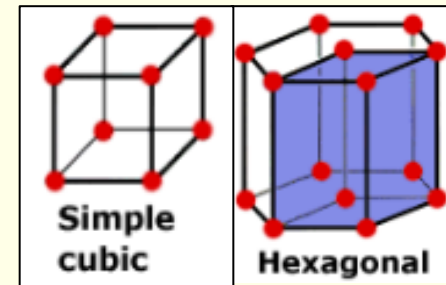
- **(104)** and **(110)** planes in Fe_2O_3 , **(311)** plane was used in Fe_3O_4 .

- Bragg's law: $d = \frac{n\lambda}{2\sin\theta'}$

- Hexagonal closed – packed crystal: $\frac{1}{d^2} = \frac{4}{3} \times \frac{h^2+k^2+hk}{a^2} + \frac{l^2}{c^2}$

- Cubic close – packed crystal: $\frac{1}{d^2} = \frac{h^2+k^2+l^2}{a^2}$

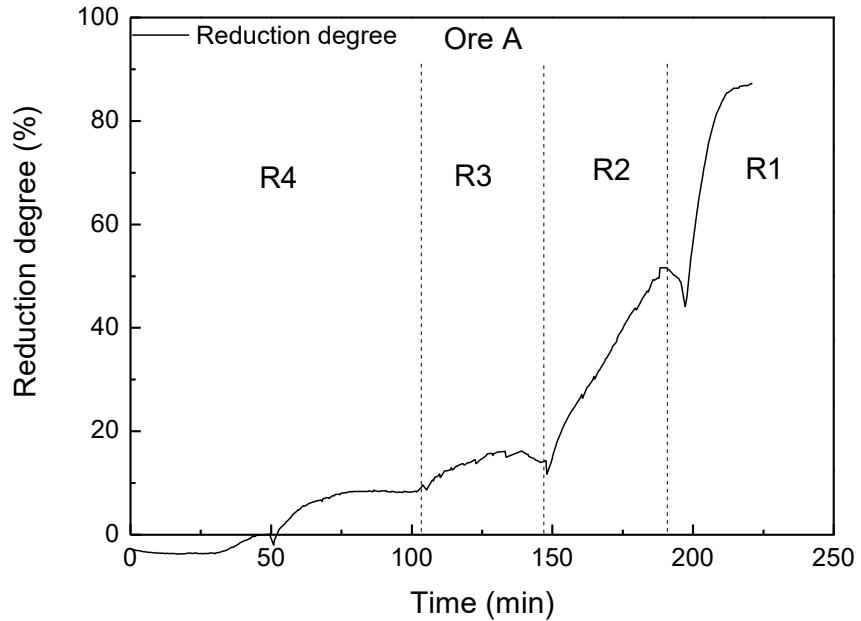
- d is the interplanar spacing, a and c are the lattice constants, $\{hkl\}$ is the crystal plane, n is the diffraction order, taken as 1 in this study



3. Results and discussion

3.1. Reduction behavior of four kinds of iron ores and their kinetic analyses

□ Reduction behavior of **four iron ores**



Change in reduction degree of Ore A at four-stage reduction

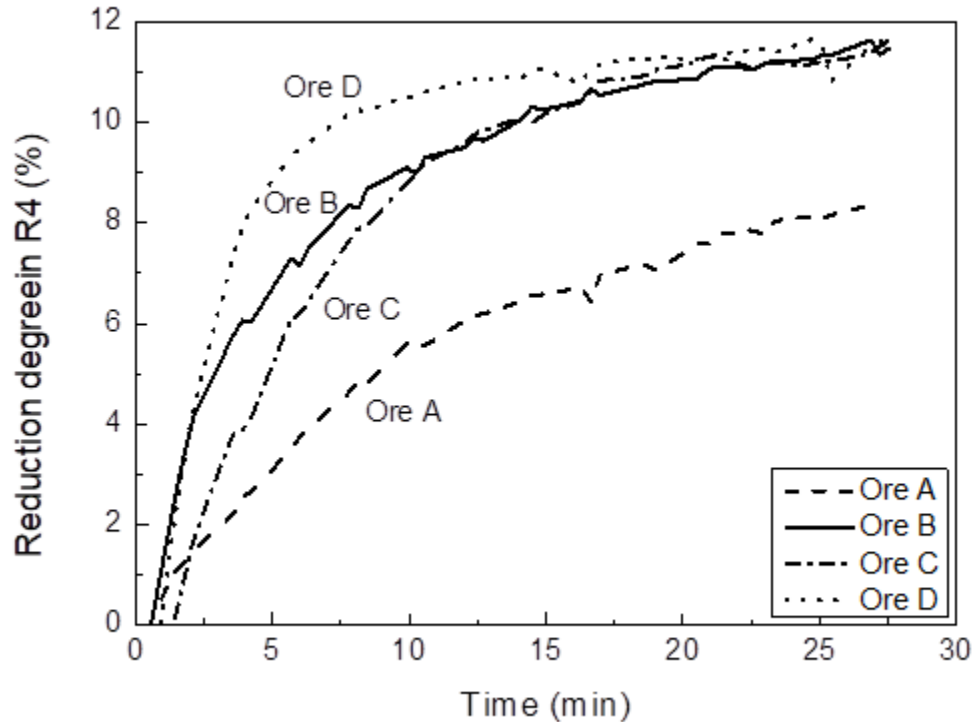
Reduction degree in each stage (%)				
Iron ores	R4	R3	R2	R1
Ore A (Carajas)	9	16.7±0.6	52.3±0.6	89±1
Ore B (MAC)	11	15.6±0.6	37.6±1.1	80±1
Ore C (Royhill)	11	15.6±0.6	37.4±0.7	81±0.6
Ore D (Yandi)	11	17±1	33.7±2.0	73.3±1.2

- ✓ The final reduction degree of **Ore A (Carajas)** was measured to be **89% as the highest**.
 - ✓ **Ore B (MAC)** and **Ore C (Royhill)** showed similar reduction degrees of **81 %**. **Ore D (Yandi)** exhibited the lowest degree of final reduction of **73 %**.
- ⇒ Difference in reduction behavior of four iron ores become noticeable starting from R2 reduction stage.

3. Results and discussion

3.1. Reduction behavior of four kinds of iron ores and their kinetic analyses

Reduction behavior at R4 stage



Reduction behavior of four iron ores at R4

Specific surface areas after dehydration (m²/g)

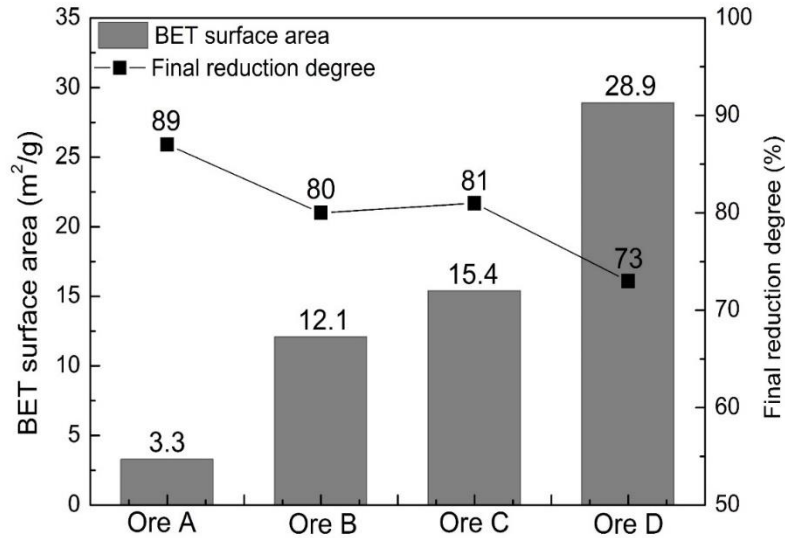
Ore A	Ore B	Ore C	Ore D
2.8	11.9	12.3	27.7

- ✓ At **R4** stage, **Ore A (Carajas)** showed not only the **smallest reduction degree**, but also **lower reduction rate** at R4 while **Ore D (Yandi)** showed the **highest** reduction rate.
- ✓ The iron ores containing **Fe₂O₃·H₂O** and **FeO(OH)** showed **higher surface areas**, which indicates the **formation of pores** due to dehydration. A slower reduction rate was observed for lower surface area, suggesting that the **reduction reaction at R4 might be diffusion control**.

3. Results and discussion

3.1. Reduction behavior of four kinds of iron ores and their kinetic analyses

Reduction behavior during R2 and R1 stage



Relationship between surface area after R3 reduction and final reduction degree

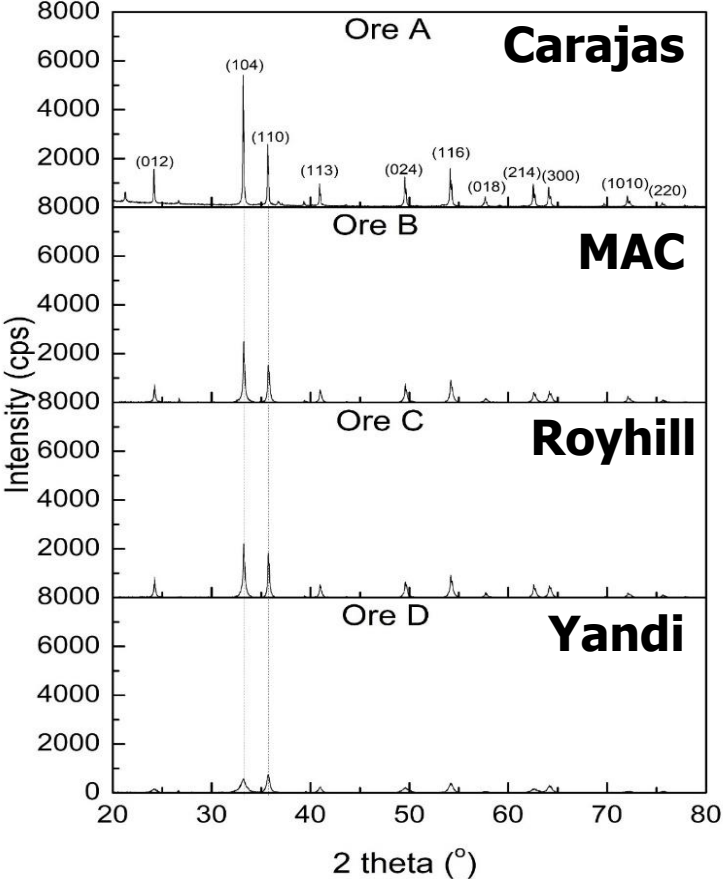
- ✓ The **surface area is not clearly correlated** with the final reduction degree. Conversely, **Ore D(Yandi) showing the highest surface area** was measured to reach the **lowest final reduction degree**.
 - ⇒ This might indicate that **different reduction mechanisms** might apply to the reduction in **wustite to metallic iron at R2 and R1**.
 - ⇒ The reduction mechanism was measured to be **1st order and 3rd order chemical reaction for R2 and R1**, respectively.

Model		R ² value for each model		
		R4	R2	R1
Phase-Boundary control Geometrical Contraction	Mass Transport	0.9096	0.9938	0.8406
	Contracting Area	0.9125	0.9966	0.8914
	Contracting Volume	0.9134	0.9968	0.9064
Diffusion Control	1-D Diffusion	0.9811	0.9918	0.8790
	2-D Diffusion	0.9820	0.9863	0.9121
	3-D Diffusion – Jander	0.9829	0.9784	0.9466
	3-D Diffusion – Ginstling	0.9823	0.9838	0.9255
Reaction Control	First Order	0.9152	0.9971	0.9326
	3/2 Order	0.9180	0.9951	0.9619
	Second Order	0.9206	0.9909	0.9791
	Third Order	0.9259	0.9759	0.9835
Nucleation	Avrami 1.5	0.8704	0.9943	0.9137
	Avrami 2	0.8432	0.9901	0.9029
	Avrami 3	0.8130	0.9839	0.8911
	Avrami 4	0.7968	0.9801	0.8848

3. Results and discussion

3.2. Effect of crystallite size and lattice constant on the reduction behavior of iron ores

Crystallite size and lattice constant after dehydration (Fe_2O_3)



Phase analyses of iron ores after dehydration

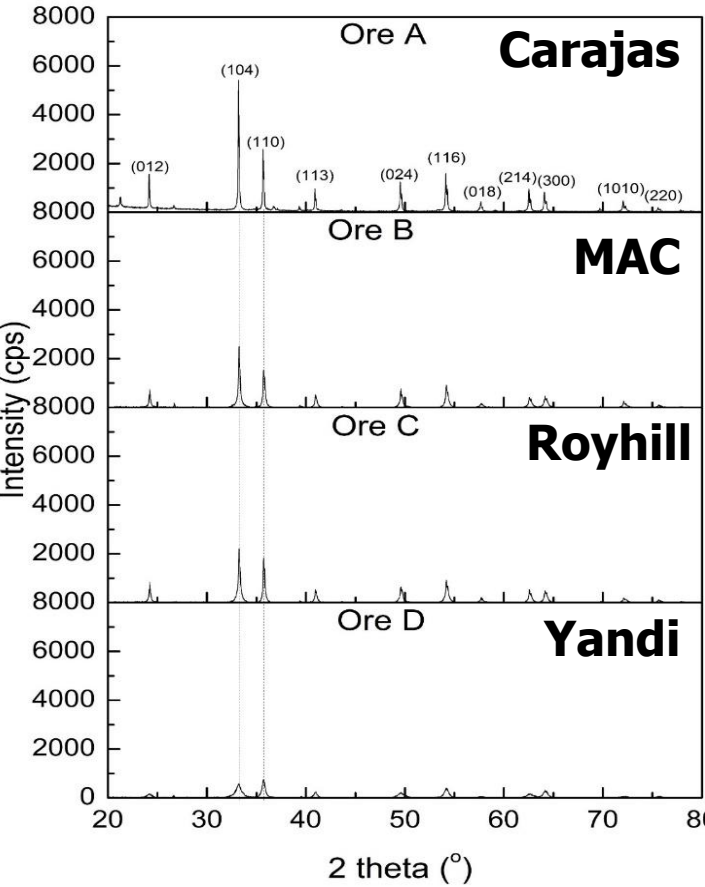
Iron ores	Lattice constant (Å)		Crystallite size (Å)
	a=b	c	
Ore A (Carajas)	5.026	13.752	18.293
Ore B (MAC)	5.018	13.713	8.651
Ore C (Royhill)	5.018	13.713	7.946
Ore D (Yandi)	5.018	13.713	2.559

- ✓ For all the iron ores, the **lattice constant of Fe_2O_3 showed similar values**, which matched the results mentioned in the previous study. However, the **crystallite size are significantly different** for the iron ores.
- ✓ **Ore D** showed the **lowest degree of final reduction** showed the **smallest crystallite size**. These **results are in opposite to those reported** in the previous investigation.
 - The **previous study** explained the reduction **mechanism of nickel oxide by diffusion control**, which **suggested that smaller crystallite size would prefer to be reduced**.

3. Results and discussion

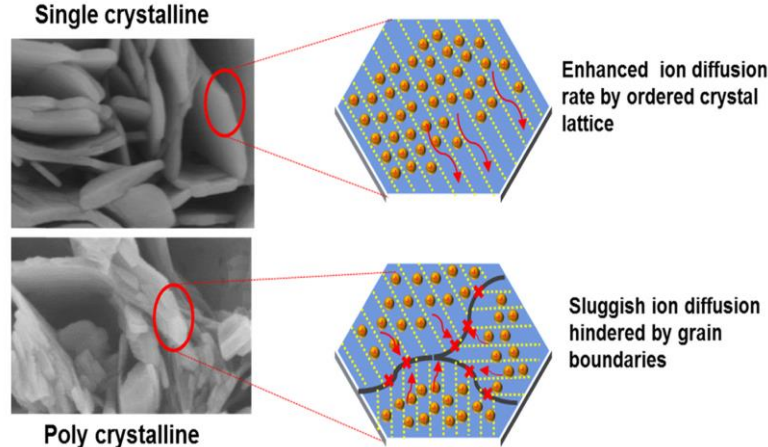
3.2. Effect of crystallite size and lattice constant on the reduction behavior of iron ores

Crystallite size and lattice constant after R3 (Fe₃O₄)



Phase analyses of iron ores after dehydration

Iron ores	Lattice constant (Å)	Crystallite size (Å)
	a=b=c	(311)
Ore A	8.376	6.809
Ore B	8.341	3.471
Ore C	8.341	3.339
Ore D	8.341	2.983

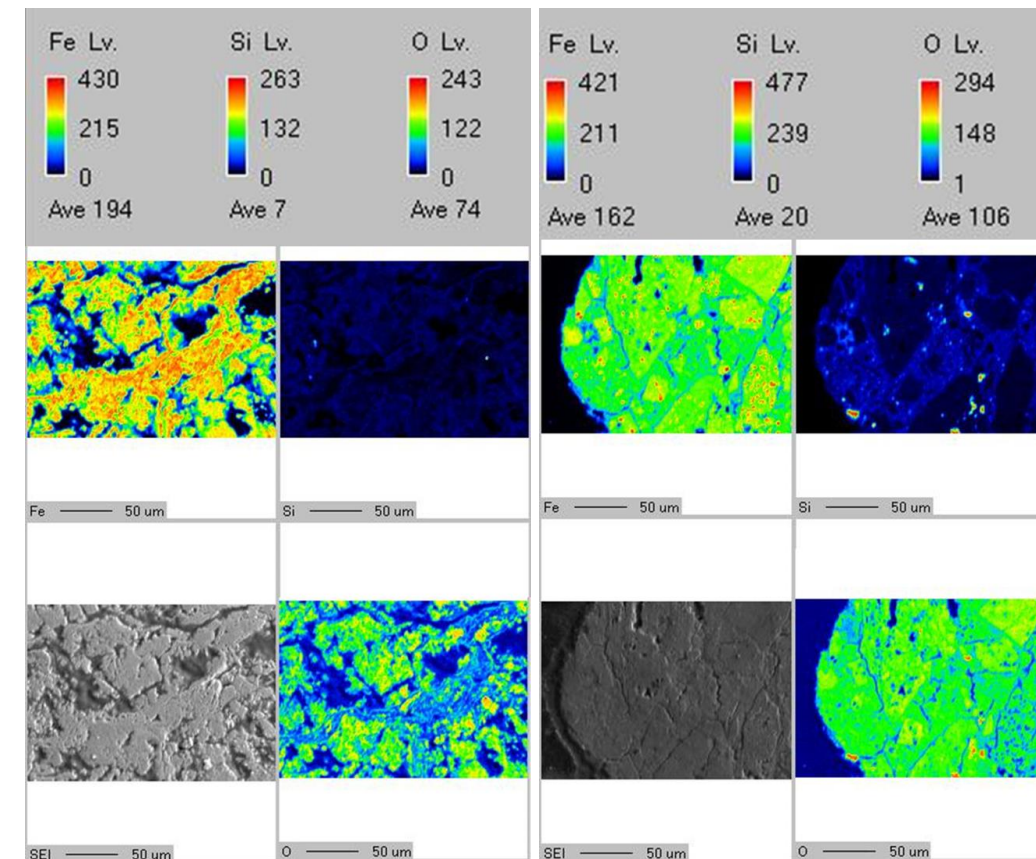


- ✓ Lattice size of magnetite was consistently estimated to be similar within all iron ores while the **crystallite size of the iron ores showed different** values.
 - ✓ The **order of crystallite size** in magnetite showed **the similar trend** to those in hematite.
 - This might be attributed to **impurities such as SiO₂ and MgO**, as mentioned in previous studies.
 - Previous studies mentioned that **impurities induce defects and distortions** of crystal **structure**.
- ⇒ The current study observed the variation in SiO₂ content for the iron ores, and the **crystallite size was found to be inversely proportional to SiO₂ content** in the iron ores.

3. Results and discussion

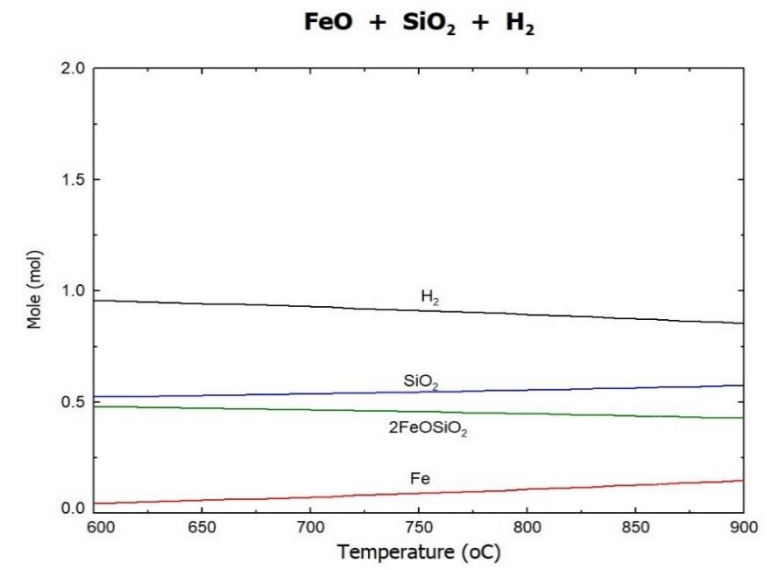
3.3. Effect of SiO₂ on the reduction behavior of iron ores

□ Distribution of Si and Fe (EPMA) after R2 reduction



Ore A (Carajas)

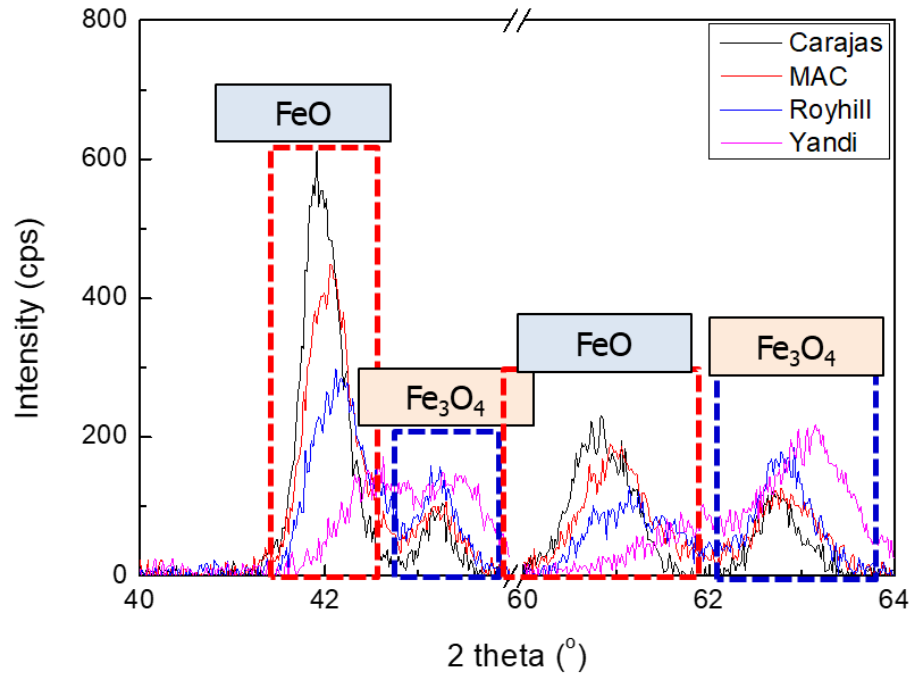
Ore D (Yandi)



- ✓ It was observed that there was more **overlapping** area in the distribution of **Fe and Si in Ore D(Yandi)** compared with **Ore A(Carajas)**.
⇒ It is believed that **SiO₂ reacts with wustite to form fayalite** during reduction.
- ✓ Thermodynamic calculation was performed using FactSage to confirm whether **fayalite might form in the reducing atmosphere** in the temperature range of **600 to 900 °C**.

3. Results and discussion

□ XRD analysis of wustite after reduction



Comparison of XRD peaks for reduced iron ores:

(a) In the range of 41 to 44 degree

(b) In the range of 60 to 64 degree

- ✓ As the content of **SiO₂ within the iron ores increases**, it could be observed that XRD peaks shift **towards the right side**.
- ✓ Shift in peak positions was observed, suggesting that **gangue components react with FeO**, leading to the change in structure.

4. Conclusions

- ✓ As the **surface area increased** due to the **dehydration** of iron ore, the **reduction rate in R4 increased**.
 - This result was consistent with the reaction mechanism of R4 stage, which was analyzed to be **controlled by diffusion**.
- ✓ However, **no correlation** was observed between the **final reduction degree** and **surface area** of iron ore.
 - This suggests that **reduction mechanism other than diffusion** operates in the later stage of reduction.
- ✓ The **final reduction degree decreased** as the **gangue content** in iron ore **increased** and **crystallite size** of iron oxides **became smaller**.
 - As the **crystallite size decreases**, the **diffusion of hydrogen within lattice** is expected to be **hindered**, leading the reduction reaction less favorable.
 - **Increase in gangue** content **promotes the formation** of phases such as **fayalite**, which are **challenging to reduce**, thereby **suppressing the reduction** reaction.